International Journal of Thermal Sciences 48 (2009) 1884–1893

Contents lists available at ScienceDirect

International Journal of Thermal Sciences

journal homepage: www.elsevier.com/locate/ijts

Inlet conditions effects on vertical wall jets in forced and mixed convection regimes

Ameni Mokni [a], Jamel Kechiche [a], Hatem Mhiri [a], Georges Le Palec [b,*], Philippe Bournot [b]

[a] Unité de Thermique et Environnement, Ecole Nationale d'Ingénieurs de Monastir, Route de Ouardanine, 5000 Monastir, Tunisia
[b] IUSTI UMR CNRS 6595, Technopôle de Château-Gombert, 5 rue Enrico Fermi, 13013 Marseille Cedex 20, France

ARTICLE INFO

Article history:
Received 24 September 2007
Received in revised form
13 January 2009
Accepted 27 February 2009
Available online 26 March 2009

Keywords:
Laminar
Wall jet
Heat flux
Inlet conditions
Convection
Prandtl number

ABSTRACT

In this paper a numerical investigation of a laminar isothermal or nonisothermal two dimensional plane wall jet is carried out. Special attention has been paid to the effect of the inlet conditions at the nozzle exit on the hydrodynamic and thermal characteristics of the flow, in both convection regimes: forced and mixed. Two velocities profiles at the nozzle exit are used: uniform profile and parabolic profile. The Prandtl number effect on the jet flow characteristics is also analyzed in the case of forced convection regime.

The system of governing equations is solved with an implicit finite difference scheme. For numerical stability we use a staggered non-uniform grid. The obtained results show, for the two convection modes, that the inlet conditions affect the flow in the immediate neighbourhood of the nozzle (core region) in which the flow is governed mainly by the inertia forces. In the established region the results become independent of the flow inlet conditions. Secondly, the effect of the Prandtl number is significant in the plume region in which the jet flow is governed by buoyant forces.

1. Introduction

Due to the diversity of their aspects and their applications, typical jet flows represent a constant interest. Indeed, they are widely used in many industrial applications, such as jet cutting, cooling through impingement, heat insulation, inlet devices in ventilation, separation control in airfoils and film cooling of turbine blades [1].

The wall jet in which the flow is injected tangentially to a plane plate at high velocity, the inner wall boundary jet and the outer free jet attracted much attention of researchers as indicated by an abundant literature [2–21] on related subjects. In these studies [2–16] both hydrodynamic and thermal characteristics of the flow have been investigated in order to know the local coefficient of heat transfer.

In such plane wall jets, we distinguish the zone of the boundary layer which lies between the wall and the maximum velocity line and the external zone that behaves like a free jet [2,3]. Former works were concerned with this type of flows but most of them [2–8] treated the turbulent case, due to its practical interest for industrial applications. Nevertheless laminar wall jets are widely used in various industrial and domestic applications such as the filling and the cleaning of the surfaces coating by air flow and continuous lubrication of the contact of solid surfaces in order to avoid wear.

In turbulent mode Nizou [2] and then Nizou and Tida [3] proposed an analytical formulation for the parietal friction coefficient as a function of the longitudinal distance of the flow. This leads to the deduction of an analogy between the transfer of heat and momentum for a turbulent wall jet. Leduc and Jaumotte [4] proposed numerical solutions related to the thermal transfer between a jet in forced convection and a plane plate subjected to a constant heat flux. Launder and Spalding [5] established the system of equations recommended for high Reynolds numbers. Ljuboja and Rodi [6] showed that this model presents limitations for the wall jet and proposed a modified version of the k–ε model.

Recently Kechiche et al. [7,8] studied the influence of the velocity and temperature conditions at the nozzle exit on the turbulent dynamic and thermal parameters of the flow. For the case of an isothermal wall jet, they showed that these conditions do not have an influence on the flow parameters in the established area of the flow. They also showed that in the case of an air blast evolving tangentially with a plate subjected to a constant heat flux in forced convection, the velocity profile at the nozzle exit does not have an

* Corresponding author. Tel.: +33 491113842; fax: +33 491113879.
E-mail address: georges.lepalec@univmed.fr (G. Le Palec).

1290-0729/$ – see front matter © 2009 Elsevier Masson SAS. All rights reserved.
doi:10.1016/j.ijthermalsci.2009.02.021

Nomenclature

b	width of the nozzle m
C_f	friction coefficient $C_f = 2\tau_p/\rho u_m^2$
C_p	specific heat at constant pressure J kg^{-1} K^{-1}
Fr	Froude number Fr $= u_0^2\lambda/g\beta\phi b^2$
g	gravitational acceleration m s^{-2}
Gr	Grashof number Gr $= g\beta\phi b^4/\nu^2\lambda$
h	local heat transfer coefficient W m^{-2} K^{-1}
ℓ	length of the heated vertical plate m
L	dimensionless length of the heated vertical plate
Nu_x	local Nusselt number $Nu_x = hx/\lambda$
Pr	Prandtl number Pr $= \upsilon/\alpha$
Re	Reynolds number Re $= bu_0/\upsilon$
St	Stanton number St $= Nu_{x2}/Re_{x2}Pr^{1/3}$
T	temperature K
u,v	streamwise and transverse components of velocity, respectively m s^{-1}
U,V	dimensionless streamwise and transverse components of velocity, respectively
x,y	streamwise and transverse coordinates, respectively m
X,Y	dimensionless streamwise and transverse coordinates, respectively
X_1	dimensionless virtual origin
X_2	modified dimensionless coordinate $X_2 = X + X_1$
x_1	position of the fractious origin

Greek symbols

α	thermal diffusivity of the fluid m^2 s^{-1}
β	coefficient of thermal expansion K^{-1}
θ	dimensionless temperature
λ	thermal conductivity of the fluid W m^{-1} K^{-1}
υ	kinematic viscosity $\upsilon = \mu/\rho$ m^2 s^{-1}
ρ	fluid density kg m^{-3}
τ	Wall shear stress $\tau = \mu(\partial u/\partial y)_{y=0}$ Pa
ϕ	Wall heat flux W m^{-2}

Indices

m	maximum value
p	wall value
x	local value
x_2	Local modified value
∞	external (ambient conditions value)
0	initial value of jet at exit of the nozzle

influence on the thermal transfer between the plate and the flow in the thermal established region. A decrease in the Reynolds number produces a decrease in the convective thermal transfer.

An examination of the literature reveals that in laminar mode; most of the studies limit themselves to analytical solutions or a numerical resolution using a change of variables ignoring the conditions at the nozzle exit [9–16]. We can quote for example, Schlichting [9] and Gorla [10]: these authors analyzed mainly the established zone of the jet while basing themselves on the momentum conservation and on the fact that, in the mixture zone, the inertia forces are dominating the buoyancy forces.

Following the work of Savage and Chan [11] who separately studied the area of the jet and that of the plume, Wilks and Hunt [12], by using a more adequate variables change, proposed numerical results for the three regions of a plane wall jet: exact analytical solutions for the forced convection in the vicinity of the nozzle and for the natural convection far from the emission section were deduced.

Yu et al. [14] studied numerically a laminar wall jet by introducing new parameters and a variables change which replace the two initial forms of the velocity and temperature profiles at the nozzle exit. These conditions were replaced by two integration constraints expressing the momentum and energy conservation of the flow discharged by the nozzle.

Later Mhiri et al. [17] were interested in the effect of the emission conditions at the exit of the nozzle on isothermal and non-isothermal laminar wall jet. They considered two emission conditions verifying the constraints suggested by Yu et al. [14]. They showed that in the case of a laminar wall jet these conditions do not have any influence on the flow in the plume zone, where the buoyancy forces are dominating. This zone depends only on the Reynolds and Grashof numbers; it is reached at a distance $x/b = 10(Re^{11}/Gr^4)^{1/7}$.

Marzouk et al. [18] studied numerically the influence of an initial disturbance on dynamic and thermal parameters of a pulsed laminar wall jet. They used two wall thermal conditions: adiabatic or isotherm. They showed that for flow pulsation amplitude of 10% and a Strouhal number of 0.3, an increase of 8% in the thermal transfer is obtained.

Recently the heat transfer problem between a two-dimensional laminar horizontal plane jet and a rectangular slab has been solved by Kanna and Das [19]: they found solutions for the local Nusselt number, the average Nusselt number and the interface boundary temperature. They used a conjugate boundary condition for the wall temperature which was determined by coupling the energy equations in the fluid with that of the slab through the interface between fluid and slab. They showed that for $Pr \ll 1$, heat exchange depends on $Re^{3/4}$, Pr, the thermal conductivity and the aspect ratio of the slab; while for $Pr > 1$, the relevant parameter set is $Re^{3/4}$, $Pr^{1/3}$, the thermal conductivity and the slab aspect ratio. However, the size of the calculation domain is limited to $20\,b \times 40\,b$, b being the width of the nozzle. A more recent study was carried by Kumar Raja et al. [20] who studied numerically the transient flow of buoyancy assisted mixed convection in wall jet. The main purpose of their work is to study the effects of the Prandtl and Grashof numbers in transient mixed convection on a wall jet heated by the wall and cooled by the ambient fluid. They showed that the time required for the average Nusselt number to reach a steady-state value decreases with increasing Grashof number.

This work is devoted to the special case of vertical laminar wall jets. We propose to investigate the influence of the exit nozzle conditions on the evolution of dynamic and thermal characteristics of the jet: two velocity profiles, uniform and parabolic, are tested at the exit of the nozzle. First, we study the influence of these profiles on the heat transfer for an isothermal wall jet and forced convection. In a second part, the behaviour of various fluids evolving in forced convection near a vertical plate plane is analyzed, by varying the Prandtl number. The last stage is devoted to the influence of the emission conditions on the heat transfer for a vertical wall jet under the mixed convection regime.

2. Assumptions and governing equations

2.1. Assumptions

We consider an incompressible laminar jet resulting from a rectangular nozzle into a quiescent surrounding fluid. The nozzle thickness is smaller compared to its width so that edge effects are

negligible; thus the problem can be considered two dimensional. The experiment shows that the static pressure undergoes a very weak variation, so we consider it constant in the jet. Both mixed and forced convection regimes are considered by using the Boussinesq approximation in which the density varies linearly with temperature in the buoyancy term of the momentum conservation equation. The geometry and the coordinates system used are shown in Fig. 1.

2.2. Governing equations

Under the above assumptions, the governing equations describing the behaviour of a vertical buoyant wall jet flow are:

$$\frac{\partial u}{\partial x}+\frac{\partial v}{\partial y}=0 \tag{1}$$

$$u\frac{\partial u}{\partial x}+v\frac{\partial u}{\partial y}=\upsilon\frac{\partial^2 u}{\partial y^2}-\varepsilon g\beta(T-T_\infty) \tag{2}$$

$$u\frac{\partial T}{\partial x}+v\frac{\partial T}{\partial y}=\frac{\lambda}{\rho C_p}\frac{\partial^2 T}{\partial y^2} \tag{3}$$

Where $\alpha=\lambda/\rho C_p$,

ε takes value 0 in the case of an isothermal jet, and 1 when it is a heated jet.

These equations are completed by the following set of boundary conditions:

$$x=0\begin{cases}0<y<b:\ u=u_0;\ v=0;\ T=T_0;\\ y\geq b:\ u=0;\ v=0;\ T=T_\infty;\end{cases}$$

$$x>0\begin{cases}y=0:\ u=0;\ v=0;\\ \textit{Wall submitted to uniform heat flux}\left(\frac{\partial(T-T_\infty)}{\partial y}\right)_{y=0}=-\frac{\phi}{\lambda};\\ y\to\infty:\ u=0;\ T=T_\infty;\end{cases} \tag{4}$$

By using the following dimensionless variables:

$$X=\frac{x}{b};\ Y=\frac{y}{b};\ U=\frac{u}{u_0};\ V=\frac{v}{u_0}\ and\ \theta=\frac{T-T_\infty}{\phi\cdot b}\lambda \tag{5}$$

these equations become, in their dimensionless form:

$$\frac{\partial U}{\partial X}+\frac{\partial V}{\partial Y}=0 \tag{6}$$

$$U\frac{\partial U}{\partial X}+V\frac{\partial U}{\partial Y}=\frac{1}{Re}\frac{\partial^2 U}{\partial Y^2}-\varepsilon\frac{\theta}{Fr} \tag{7}$$

$$U\frac{\partial \theta}{\partial X}+V\frac{\partial \theta}{\partial Y}=\frac{1}{RePr}\frac{\partial^2 \theta}{\partial Y^2} \tag{8}$$

The associated dimensionless boundary and inlet conditions become:

$$X=0\begin{cases}0<Y<1:\ V=0;\ \theta=0;\\ \textit{Uniform profile}: U=1;\\ \textit{Parabolic profile}: U=(180)^{1/3}\left(Y-Y^2\right);\\ Y\geq 1:\ U=0;\ V=0;\ \theta=0;\end{cases}$$

$$X>0\begin{cases}Y=0:\ U=0;\ V=0;\\ \textit{Wall submitted to uniform heat flux}: \left(\frac{\partial\theta}{\partial Y}\right)_p=-1;\\ Y\to\infty:\ U=0;\ \theta=0;\end{cases} \tag{9}$$

3. Numerical method

Boundary layer equations, associated with the boundary conditions and the assumed velocity profiles at the exit of the nozzle were solved by a finite difference method. A shifted rectangular grid superposed on the field of the flow is used, as shown in Fig. 1. The continuity equation is discretized at nodes $(i+½, j+½)$ whereas momentum and energy equations are discretized at nodes $(i+½, j)$. A non-uniform grid is used in the X direction of the flow. The calculation step is very small in the vicinity of the nozzle $(\Delta X=10^{-4})$ then it increases as one moves away in the jet $(\Delta X=10^{-1})$. In the transverse direction the calculation step is

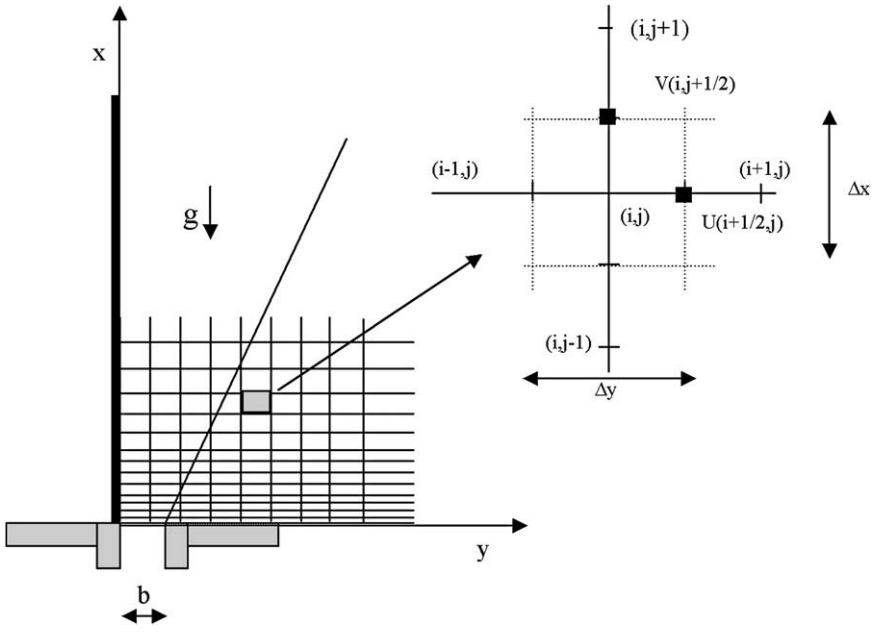

Fig. 1. Coordinate system of the configuration flow.

considered constant ($\Delta Y = 2.10^{-2}$). Calculations begin on the leading edge of the plate ($X = Y = 0$) and are performed according to the fluid flow's direction. The obtained discretized equations are solved by adopting a non linear Gauss Siedel method, which is a successive approximating method. This method, which was successfully used in former works [22–24], was adopted for numerical stability reasons, compared to methods using a non staggered grid discretization. The convergence of the solution is reached when the relative change of U between two successive iterations is less than 10^{-7} for each node of the field.

4. Results and discussion

The results obtained from numerical integration of the equations are presented for the two following velocity profiles at the nozzle exit: uniform profile and parabolic profile.

4.1. Vertical wall jet in forced convection

We consider an incompressible jet issuing tangentially to an infinite flat plate from a rectangular nozzle. The temperature of the fluid at the exit of the nozzle is constant and equal to the ambient conditions one. The Prandtl number is 0.71 (air).

4.1.1. Dynamic study

4.1.1.1. Determination of the fictitious origin of the jet. Initially, a dynamic study of the flow was established. Previous studies [2,3,8] showed that the behaviour of the region located between the wall and the maximum velocity line differs notably from a traditional boundary layer flow because it evolves under an external flow action: it's a disturbed boundary layer. A thorough study shows that from a certain distance of the nozzle exit, one can represent the area occupied by the boundary layer by using a beam of straight lines which are built by using iso-velocities $U^* = u/u_m$ in which u_m is the maximum jet velocity in the considered section. This beam is defined in the area $0.7 < u^* < 1$ and all the lines reach together by the same coordinate equal to $X = -X_1$ that acts as a virtual origin.

The results show that the X_1 value is rather important and depends on the Reynolds number at the nozzle exit section, contrary to the turbulent regime [8]. This value varies between $X_1 = 160$ for $\mathrm{Re} = 500$ (Fig. 2) and $X_1 = 260$ for $\mathrm{Re} = 1500$ (Fig. 3). However we note that this variable is independent of the velocity profile at the nozzle exit section.

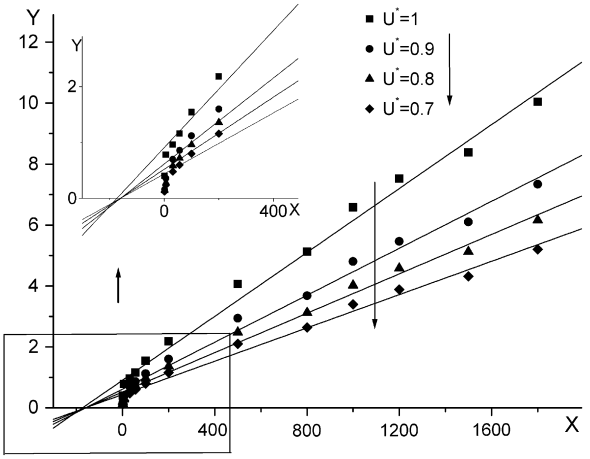

Fig. 2. Jet fictitious origin $\mathrm{Re} = 500$.

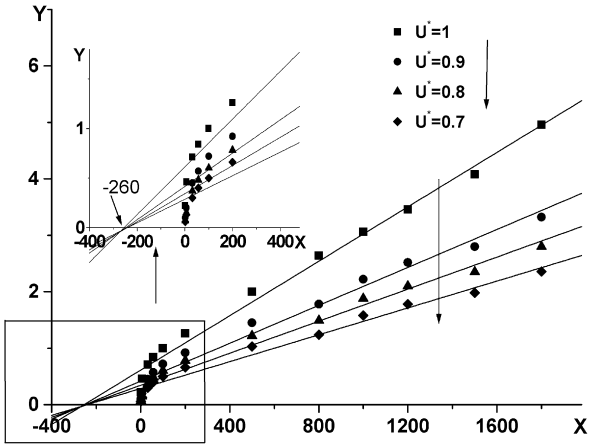

Fig. 3. Jet fictitious origin $\mathrm{Re} = 1500$.

Fig. 4 illustrates the evolution of the fictitious origin of the jet for the two velocity profiles tested at the exit of the nozzle (uniform profile and parabolic profile). It shows that this parameter follows a linear evolution within the relation:

$$X_1 = 105.4 + 0.1024\,Re \tag{10}$$

4.1.1.2. Friction coefficient. The following part will be devoted to the study of the evolution of the dimensionless friction coefficient: $C_f = 2\tau_p/\rho u_m^2$ which is given in Fig. 5 as a function of Re_{x2}, defined as:

$$Re_{x2} = \frac{u_m \cdot x_2}{\nu} = \frac{u_m(x + x_1)}{\nu} \tag{11}$$

Results are different in the vicinity of the nozzle exit, and then become perfectly similar in the plume area. Indeed, as Re_{x2} grows, the maximal x-velocity component, u_m, is less and less influenced by the inlet velocity profile: this is why all the curves tend towards the same asymptote. The slope of this line is negative because u_m vanishes as x increases, which induces a weaker wall velocity gradient and, consequently, a lower wall shear stress. This linear law can be expressed in the following form:

$$C_f = 1.28\,Re_{x2}^{-1/2} \tag{12}$$

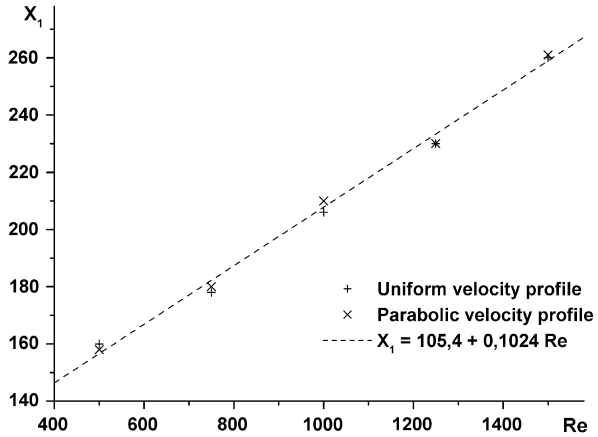

Fig. 4. Position of the jet fractious origin.

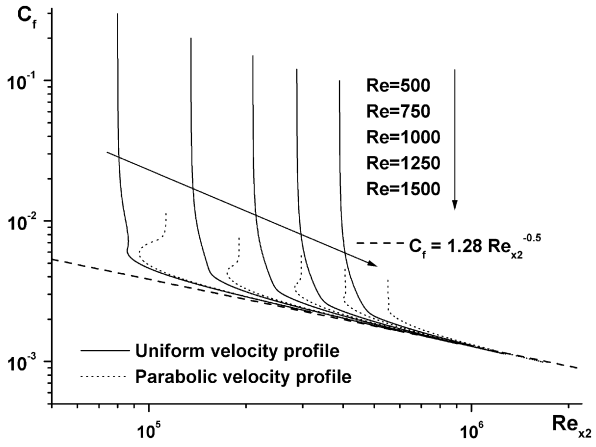

Fig. 5. Streamwise evolution of the friction coefficient.

4.1.2. Thermal study

This part is devoted to the analysis of the flow thermal aspect in order to detect the influence of the emission conditions on the heat transfer between the jet and the wall, this one being subjected to a constant heat flux. The results are presented for air ($Pr = 0.71$) and for Reynolds numbers ranging from $Re = 500$ to $Re = 1500$.

4.1.2.1. Wall temperature. We represent in Fig. 6 the dimensionless wall temperature as defined by (5) in which $T = T_p$. The limits of the three regions (jet, intermediate and plume zones) are presented with left–right arrows, which means that these limits vary with the Reynolds number.

The influence of the velocity profiles on the wall temperature is noticed only in the region close to the nozzle. Because of the sudden step in the velocity value near the nozzle exit region, the drive of ambient air by the jet is more significant when the uniform velocity profile is used. For this case, the wall temperature remains first constant and, for ascending X values, the jet expansion results in a decrease of the mean velocity so that we note an increasing temperature of the wall since this one is subjected to a constant heat flux.

In the plume region, the initial velocity profiles do not have any more an influence and the wall temperatures become identical. The evolution towards this single value results from the interaction between the friction and inertia forces. It follows that it is done more gradually with a parabolic velocity profile because near the wall, the velocity gradients are lower than those occurring when a uniform velocity profile is used.

Finally, we note that the variation of the Reynolds number does not have any influence in the jet zone; further an increase of the jet Reynolds number (Re) generates a reduction in the dimensionless wall temperature. For low Reynolds number, the dimensionless wall temperature is high. With increase in Re, convection starts dominating which implies a better cooling of the wall.

4.1.2.2. Nusselt number. The variation of the local Nusselt number along the vertical plate, Nu_x, is shown in Fig. 7, for all the cases analyzed in this study. The local Nusselt number is calculated with:

$$Nu_x = \frac{X}{\theta_p(X)} \tag{13}$$

Due to the boundary layer development along the wall, the fluid-to-wall temperature difference influences the Nusselt number. We notice that an increase of the inlet Reynolds number, Re, generates a more intense heat exchange since it results in a higher local Nusselt number. The increment in the Nusselt number increases with the Reynolds number especially in the plume region, due to the boundary layer growth. The temperature gradient is larger and results in a high Nusselt number.

These are predictable results since a high Reynolds number flows ensure a more significant driving of the surrounding fluid and consequently a higher convective heat exchange with the wall. It is also noted that the Nusselt number increases with the X distance for all the inlet conditions. In the thermally established region the inlet velocity profiles do not have any influence on the local Nusselt number evolution.

We represent in Fig. 8 the streamwise evolution of the modified local Nusselt number $Nu_{X2} = X_2/\theta_p(X) = (X + X_1)/\theta_p(X)$ according to the modified local Reynolds number Re_{X2} defined in (11). X_1 is the dimensionless virtual origin.

The convective heat exchange in the area close to the nozzle exit depends on the velocity profile and the jet Reynolds number. Further, in the thermally established region, the velocity profile do not have any influence on the evolution of the modified local Nusselt number and a correlation according to $Re_{X_2}^{0,5}$ is deduced (see below equation (15)).

In order to quantify better the overall heat exchange between the wall and the flow, we now study the evolution of the average Nusselt number defined as:

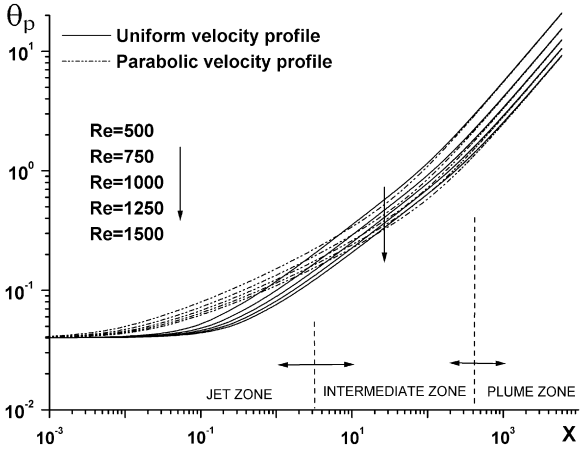

Fig. 6. Streamwise evolution of the wall temperature.

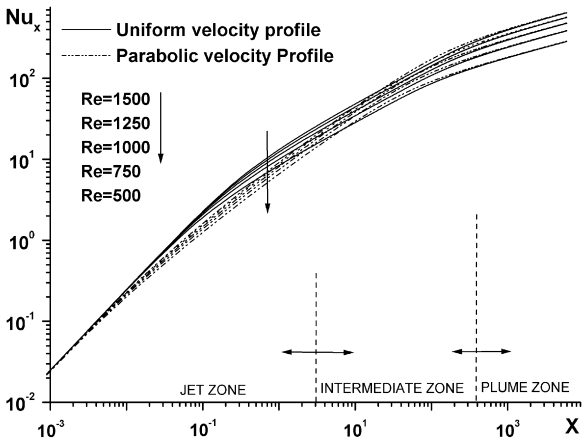

Fig. 7. Streamwise evolution of the local Nusselt number.

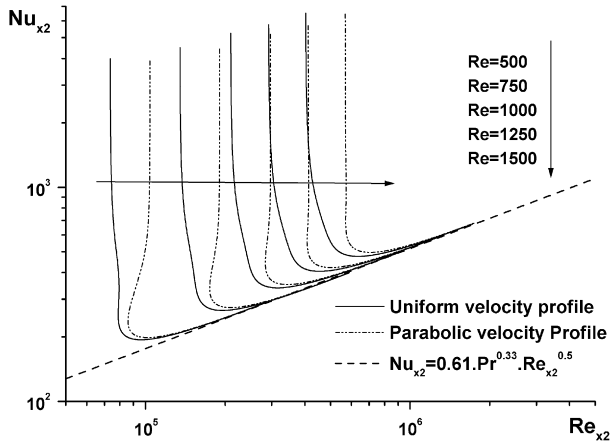

Fig. 8. Streamwise evolution of the modified Nusselt number.

$$\overline{Nu}_L = \frac{\overline{h}\ell}{\lambda},\ \ with:\ \ \overline{h} = \frac{1}{\ell}\int_0^{\ell} h_x \mathrm{d}x = \frac{1}{\ell}\int_0^{\ell} \frac{\phi}{T_p - T_\infty}\mathrm{d}x. \qquad (14)$$

L being the dimensionless streamwise length of the plate ($L = \ell/b$). Fig. 9 shows the behaviour of the average Nusselt number as function of L for several Reynolds numbers. It shows that the average Nusselt number increases with the area on which the heat flux is applied, so the fluid issued from the nozzle warms up progressively as long as it moves away from the nozzle exit. We also note the increasing of the total heat transfer when the Reynolds number increases.

For the same mass flow rate issued from the nozzle, this figure also shows that the uniform velocity profile ensures a more significant heat transfer for small lengths of the plate. Indeed, for this case, the average boundary layer thickness is lower. For lengths varying between 50 and 100 times the nozzle thickness, the velocity profile does not have any influence on the heat exchange, this value being correlated with the Reynolds number one. For higher lengths, the parabolic velocity profile ensures a slightly higher heat exchange than that obtained with a uniform profile.

4.1.2.3. Colburn analogy. The Colburn analogy is experimentally verified for laminar flow over a flat plate. In order to test the validity of the Colburn analogy in the present case, we represent in Fig. 10 the streamwise evolution of the Reynolds analogy factor: this one is

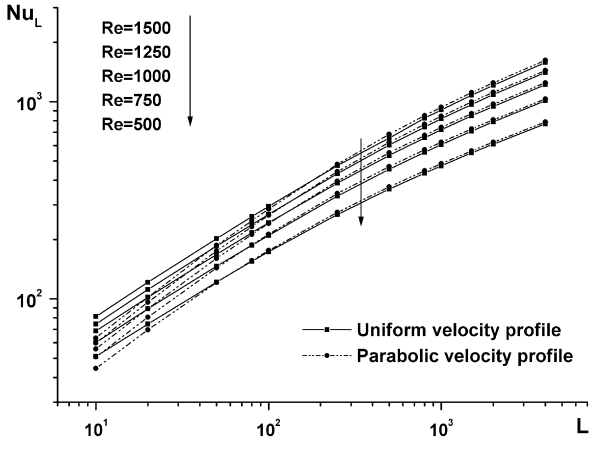

Fig. 9. Streamwise evolution of the average Nusselt Number.

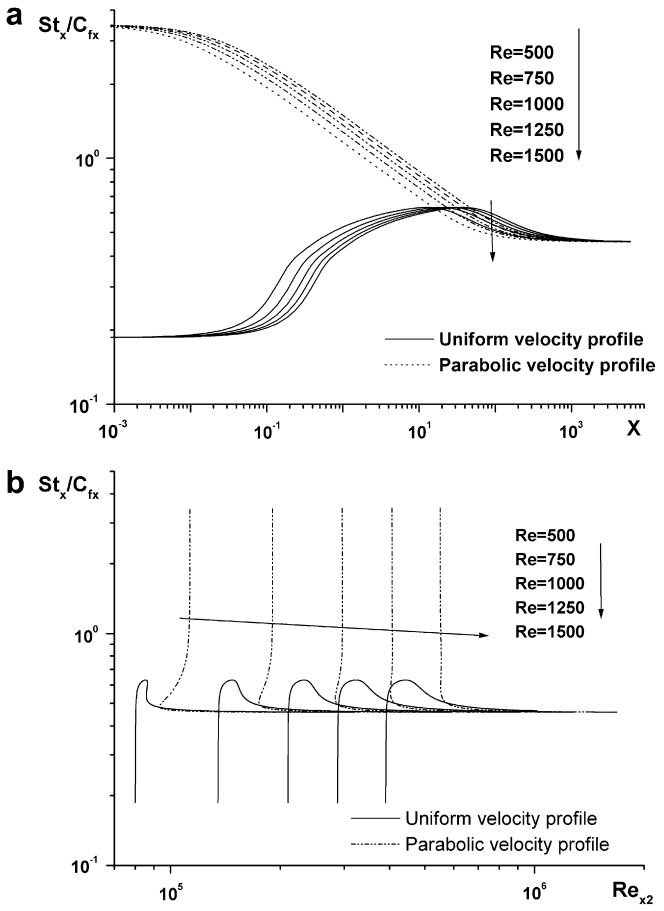

Fig. 10. a. Streamwise evolution of the Reynolds analogy factor. b. Streamwise evolution of the Reynolds analogy factor as a function of Re$_{x2}$.

defined by the ratio St/C_f where $St = Nu_{x2}/Re_{x2}Pr^{1/3}$ is the Stanton number which aims to examine the validity of the analogy between heat transfer and fluid friction for laminar forced convection. The obtained results show that a light decrease of the ratio St/C_f occurs in the thermally established region, starting from about 1000 times the nozzle width. Previous authors such as Nizou and Tida [3] and Hammond [21] showed in their experiments a light increase of this ratio. The observed differences in the values of the St/C_f ratio are reported in Table 1. This results in concluding that the Colburn analogy is not strictly applicable.

4.2. Influence of the Prandtl number on a plane wall jet in forced convection

We now consider a jet flow at the ambient temperature and ejected tangentially to a plane plate subjected to a constant heat flux in forced convection regime: in order to validate the previous study for different fluids, the heat transfer is now analyzed for Prandtl numbers ranging between 0.71 (case of the air) and 50. The average Reynolds number at the nozzle exit is Re = 1000.

Table 1
Values of the ratio St/C_f in the plume region as function of Reynolds number.

	Starting of the plume zone	End of the curve
Re = 500	0.47351	0.45801
Re = 1500	0.508	0.464

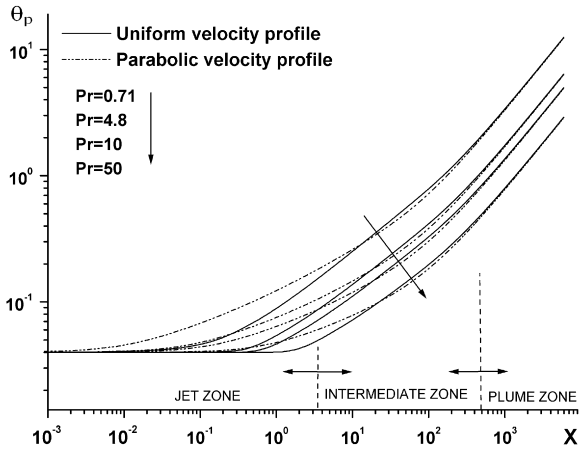

Fig. 11. Streamwise evolution of the wall temperature.

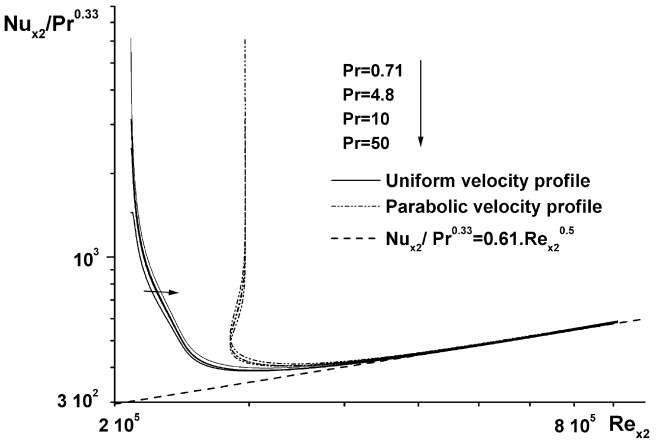

Fig. 13. Streamwise evolution of the modified Nusselt number.

4.2.1. Dynamic study

As it could be predicted with forced convection conditions, the variation of the Prandtl number has not any effect on the dynamic characteristics of the flow studied previously. Thus, for Re = 1000, the position of the fictitious origin of the jet is about 210 times the nozzle thickness for all the treated cases.

4.2.2. Thermal study

4.2.2.1. Wall temperature. Fig. 11 shows that the velocity profiles influence the wall temperature only in the region located close to the nozzle exit: indeed, in this region, the driving of ambient air by the jet is more significant with an initial uniform velocity profile which, in turn, acts on the wall heat transfer and this leads to better cooling of the plate. Further, for ascending X values, a certain agreement between the temperature curves is observed and the velocity profile have no longer influence on the wall temperature in the established zone. The boundary layer thicknesses become of the same order, leading to an equal fluid-to-wall temperature difference. It's also observed from Fig. 11 that the wall temperature decreases as the Prandtl is higher: indeed, for a fixed value of the Reynolds number, the thermal boundary layer thickness then decreases, which results in a better wall-to-fluid heat transfer and, consequently, a better cooling and a lower temperature difference between the wall and the fluid.

4.2.2.2. Nusselt number. The above observations explain the streamwise evolution of the local Nusselt number which is shown in Fig. 12. This figure shows that the heat transfer is enhanced according to the longitudinal distance and the Prandtl number. As seen previously, the heat transfer for an initial uniform velocity profile is more significant than that obtained with a parabolic profile. As a consequence of equation (13) and wall temperatures observed in Fig. 11, this difference between the results given by the two tested profiles increases with the distance from the nozzle and it is higher in the intermediate zone. In the plume zone (or established zone) this difference vanishes and becomes negligible.

Fig. 13 illustrates the evolution of the modified Nusselt number $Nu_{X2} = X_2/\theta_p(X) = (X+X_1)/\theta_p(X)$ as a function of the modified Reynolds number. This figure shows similar evolutions as those observed in the above paragraph (4.1). We notice a linear evolution starting from a modified Reynolds number of about 4.10^5. This is the beginning of the thermally established region and for the various Prandtl numbers tested, the following correlation has been verified:

$$Nu_{x2} = 0.61\, Pr^{0.33} Re_{x2}^{0.5} \tag{15}$$

Fig. 14 shows the evolution of the average Nusselt number given by $\overline{Nu}_L = \overline{h}\ell/\lambda$ according to the Prandtl number for three plate lengths: $L = 10$, 100 and 1000. For the two velocity profiles tested, we notice a linear enhance of the average Nusselt number with an increasing Prandtl number. These curves confirm the previous interpretations according to which the velocity profile influences especially the shortest plates. When the plate is sufficiently long so

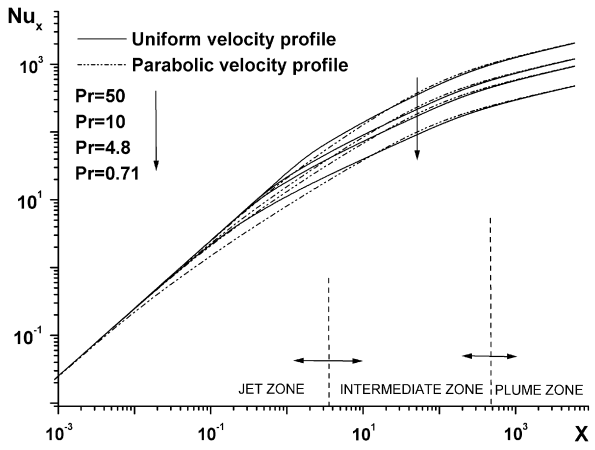

Fig. 12. Streamwise evolution of the local Nusselt number.

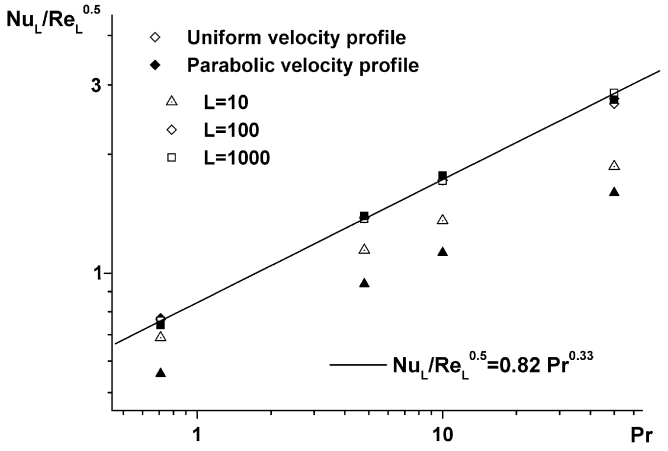

Fig. 14. Evolution of the average Nusselt number, Re = 1000.

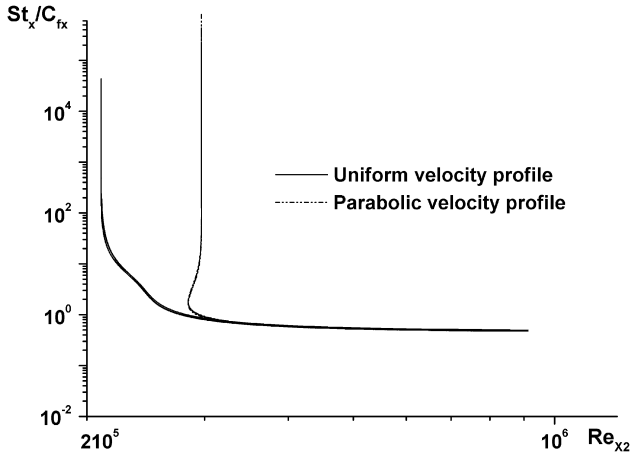

Fig. 15. Streamwise evolution of the Reynolds analogy factor.

that the plume zone can develop, and since in this region the velocity initial profiles have no longer an influence, it is possible to propose a general correlation:

$$Nu_L = 0.82\, Pr^{0,33} Re_L^{0,5} \tag{16}$$

4.2.2.3. Colburn analogy. The Reynolds analogy factor St/C_f is reported in Fig. 15 for all the Prandtl number tested and the two inlet velocity profiles. Note that all the curves merge and that the obtained results show a light decrease of St/C_f in the plume region, this last starting from about 1000 times the width of the nozzle. Thus, as in the case of Fig. 10, the Colburn analogy is not strictly applicable to laminar wall jet in forced convection regime.

4.3. Plane vertical wall jet in mixed convection

In this part we now study a wall jet issuing along a vertical plane plate subjected to a constant heat flux when gravity effects are considered, and, as above, we are interested in the influence of the emission conditions on this flow. As seen from Fig. 1, note that we examine the case of buoyancy assisted flow (buoyancy and inertia are in the same direction). The Froude number values are Fr = 2.25, 22.5, 225, 4500 and the results are presented for air (Pr = 0.71) in laminar mode (Re = 1500). For Re = 1500, these values of the Froude number correspond to Grashof numbers $Gr = 10^6$, 10^5, 10^4 and 500, respectively. A comparison of the vertical velocity profiles U with those proposed by Yu and Lin [14] is presented for three

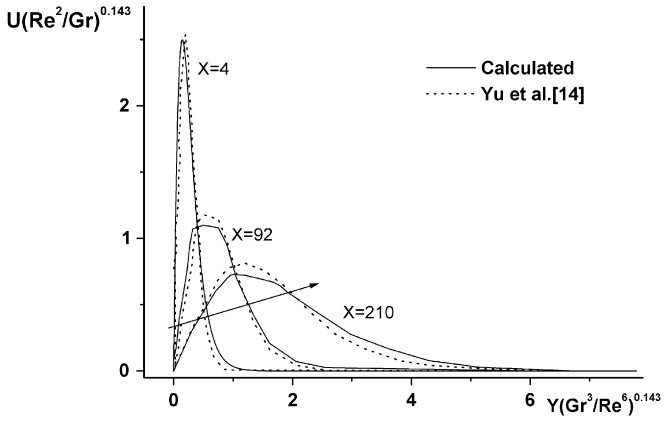

Fig. 16. Streamwise evolution of the dimensionless velocity *U*.

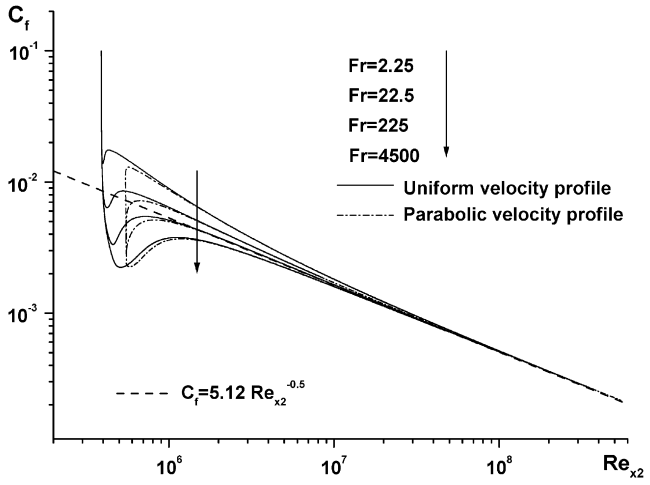

Fig. 17. Streamwise evolution of the friction coefficient.

values of *X* (Fig. 16) in order to test the validity of our numerical code. A suitable agreement is obtained.

4.3.1. Dynamic study

The variation of the Froude number does not have any effect on the dynamics characteristics of the flow, as compared to the previous cases. Thus, for Re = 1500, the position of the fictitious origin of the jet is about 260 the thickness of the nozzle for all the treated cases. The evolution of the dimensionless friction coefficient: $C_f = 2\tau_p/\rho u_m^2$ is given in Fig. 17. The results are different in the vicinity of the nozzle exit, then become perfectly similar in the plume zone, from $Re_{x2} = 5.10^7$. We notice that in this region the friction coefficient decreases in a linear way according to the relation:

$$C_f = 5.12\, Re_{x2}^{-0,5} \tag{17}$$

4.3.2. Thermal study

4.3.2.1. Wall temperature. We now focus on the streamwise evolution of the wall temperature which is shown in Fig. 18 for the two velocity profiles tested (uniform and parabolic) and for various Froude numbers. In the region close to the nozzle, the inlet velocity profile highly influences the wall temperature evolution. As one moves far from the nozzle, the difference between the obtained results decreases in the intermediate zone and becomes negligible

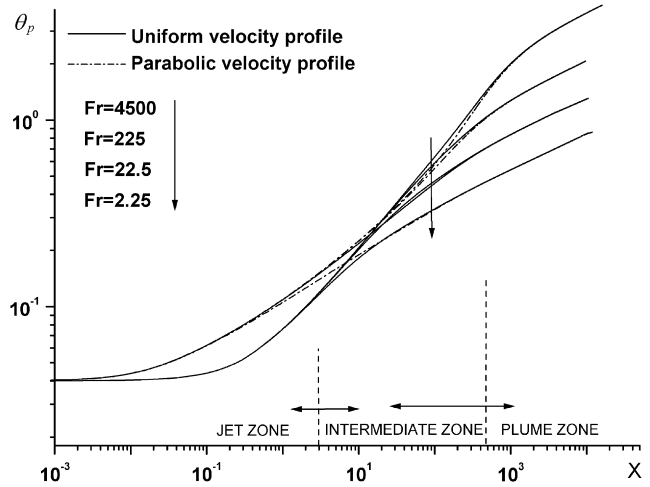

Fig 18. Streamwise evolution of the wall temperature.

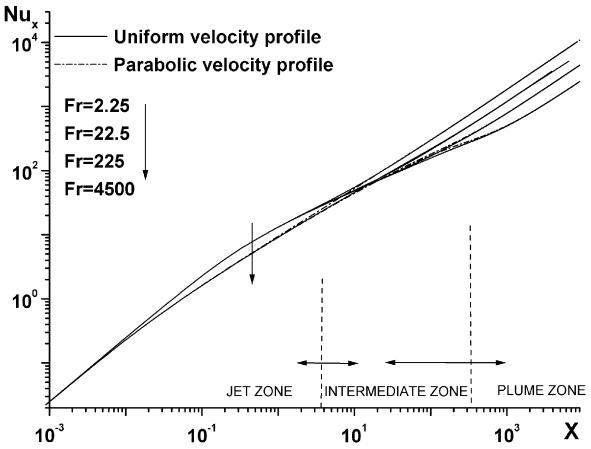

Fig. 19. Streamwise evolution of the local Nusselt number.

in the thermally established region where the inlet velocity profiles don't act any more on the wall temperature. In this last region, note the change in the slope of the profile at distances varying from about 20 times the width of the nozzle for $Fr = 2.25$ ($Gr = 10^6$) to 1000 times the width of the nozzle for $Fr = 4500$ ($Gr = 500$), which indicates that the temperature of the fluid starts to tend asymptotically towards that of the wall (the two temperatures would be equals if the plate were long enough). Indeed, the value of the Reynolds number being fixed, the buoyancy forces dominate the inertia forces at a shorter distance for the lowest Froude numbers.

4.3.2.2. Nusselt number. The evolution of the local Nusselt number is given in Fig. 19: in the vicinity of the nozzle exit the inertia forces dominate the buoyancy forces, so that the initial velocity profile influences in a significant degree the flow in this zone. The uniform profile provides a more significant flow drive and, consequently, a more significant convective heat exchange which leads to a higher Nusselt number. For greater X distances, the effect of the initial velocity profile becomes negligible, as seen in the plume region.

The fluid heating increases as the flow moves away from the nozzle. In the thermal established region the heat exchange is more significant for low Froude numbers because the buoyancy forces that are responsible of the fluid behaviour in the plume are rather significant. The thermal boundary layer on the heated wall is large for important Froude number (low Grashof number) and heat transfer is moderate. Increasing the Grashof number the boundary layer becomes more and more thin which leads to a drastic increase in the heat transfer.

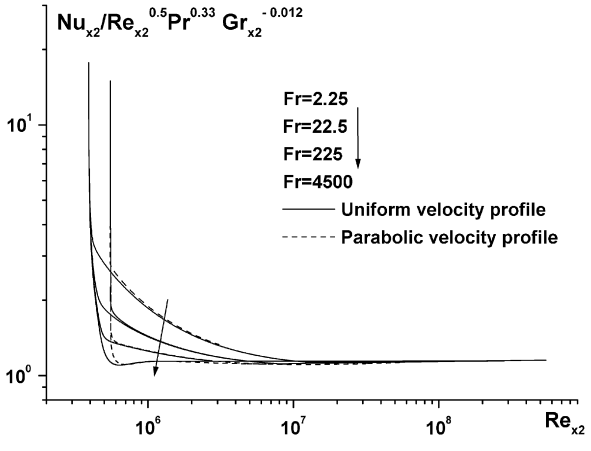

Fig. 20. Streamwise evolution of the modified Nusselt number.

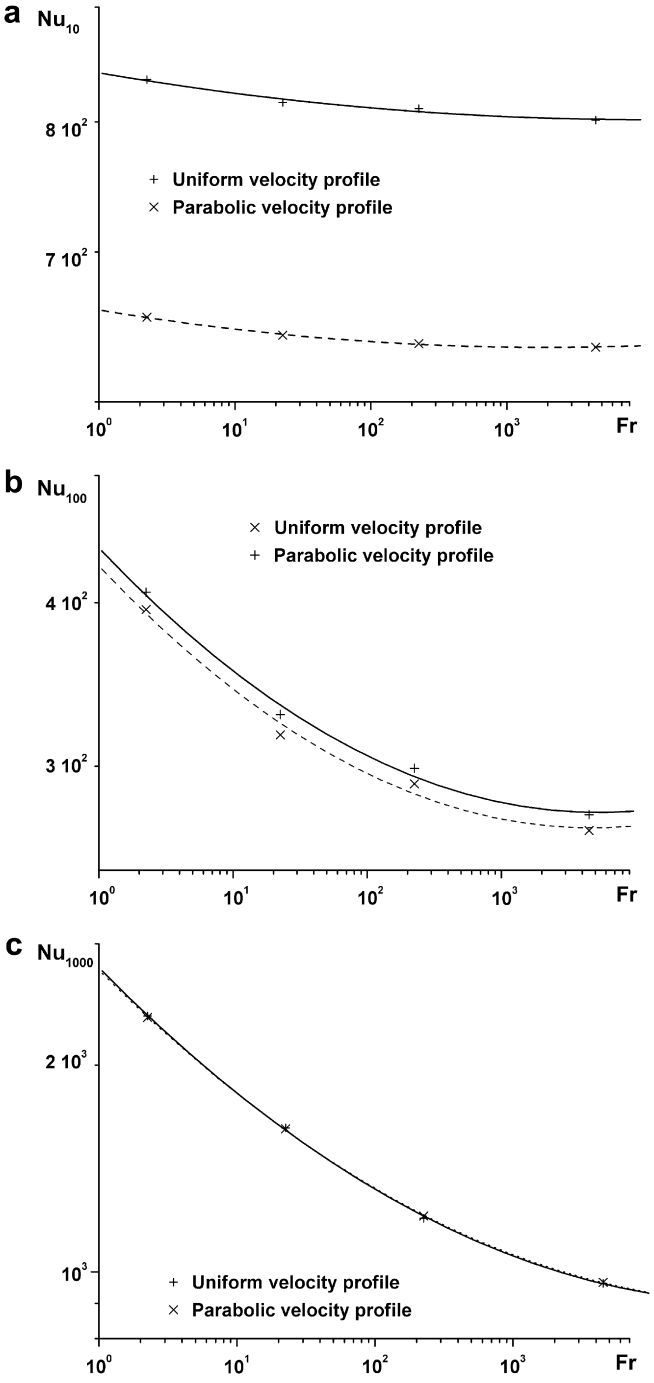

Fig. 21. a. Evolution of the average Nusselt number $L = 10$. b. Evolution of the average Nusselt number = 100. c. Evolution of the average Nusselt number $L = 1000$.

In Fig. 20, we give the streamwise evolution of modified Nusselt number $Nu_{X2} = X_2/\theta_p(X) = (X+X_1)/\theta_p(X)$ according to the modified Reynolds number $Re_{x2} = u_m \cdot x_2/\nu$.

We note a linear evolution of the modified Nusselt number in the thermally established region. This enables us to propose a correlation connecting the modified Nusselt number to the modified Reynolds number, the Prandtl number and the Grashof number:

$$Nu_{x2} = 1.14\, Pr^{0.33} Re_{x2}^{0.5} Gr_{x2}^{-0.012} \tag{18}$$

Finally, Fig. 21 shows the streamwise evolution of the average Nusselt number according to the Froude number for 3 plate lengths

: $L = 10$, 100, 1000. We deduce three correlations connecting the average Nusselt number to the Froude number varying from $Fr = 2.25$ ($Gr = 10^6$) to $Fr = 4500$ ($Gr = 500$) for each plate length. We notice that the initial velocity profile in the vicinity of the nozzle has a high effect on the value of the average Nusselt number for the shortest plates ($L = 10$); this difference decreases for higher L lengths ($L = 100$), and it completely vanishes for long plates ($L = 1000$): indeed, in the latter case, the jet and intermediate zones cover a very small area of the plate, as compared to the one covered by the plume region.

5. Conclusion

In this work we have studied laminar vertical wall jets for forced and mixed convection modes. The results relate primarily to the influence of the inlet conditions at the nozzle exit, and particularly the velocity profile. The effects of Reynolds, Prandtl and Froude numbers on the behaviour of the dynamic and thermal characteristics of the flow are discussed.

We have shown that the velocity profile at the nozzle exit highly affects the heat transfer between the jet and the heated wall in the zone of the jet: in this zone the flow is controlled by inertia forces, which imply a more significant drive of ambient fluid when a uniform velocity profile is used at the nozzle exit. In the intermediate zone, the influence of the velocity profile vanishes for the all the treated cases. Further, in the plume region, the conditions of emission have no longer influence on the flow structure.

We have also determined a correlation connecting the modified local Nusselt number according to the modified local Reynolds number. This correlation is valid in the plume zone for the two velocity profiles considered. For forced convection, we found $Nu_{x2} = 0.61\,Pr^{1/3}Re_{x2}^{1/2}$. In the case of mixed convection, the correlation becomes $Nu_{x2} = 1.14\,Pr^{1/3}Re_{x2}^{1/2}Gr_{x2}^{-0.012}$. By varying the Prandtl number, it has been verified that all the fluids react in the same manner with the variation of the conditions of emission, except that the fluid with a higher Prandtl number warms up more quickly than that with low Prandtl number. Thus we can have a more significant heat exchange with the plate. These correlations are thought to be applicable in many engineering configurations, requiring the evaluation of wall jet heat transfer coefficients.

References

[1] Conférences C.E.A., E.D.F, Phénomènes thermiques et hydrauliques non stationnaires, Jouy-en-Josas, Proc. Eyrolles Editeur, 1976.

[2] P.Y. Nizou, Analogie entre transfert de chaleur et de quantité de mouvement dans un jet pariètal plan turbulent, Int. J. Heat Mass Transfer 27 (1984) 1737–1748.

[3] P.Y. Nizou, T. Tida, Transfert de chaleur et de quantité de mouvement dans les jets pariétaux plans turbulents, Int. J. Heat Mass Transfer 38 (1995) 1187–1200.

[4] B. Leduc, A. Jaumotte, Refroidissement d'une plaque plane par jet et injection pariètaux, Revue générale de thermique 166 (1975) 692–697.

[5] B.E. Launder, D.B. Spalding, The numerical computation of turbulent flow, Comput. Meth. Appl. Mech. Eng. 3 (1974) 269–289.

[6] M. Ljuboja, W. Rodi, Calculation of turbulent wall jets with an algebric Reynolds stress model, J. Fluid Eng. 102 (1980) 350–356.

[7] J. Kechiche, H. Mhiri, G. Le Palec, P. Bournot, Numerical study of the inlet conditions on a turbulent plane two-dimensional wall jet, Energ. Convers. Manag. 45 (2004) 2931–2949.

[8] J. Kechiche, H. Mhiri, G. Le Palec, P. Bournot, Etude numérique du transfert de chaleur et de quantité de mouvement dans un jet pariètal plan turbulent, Phys. Chem. News 20 (2004) 40–48.

[9] H. Schlichting, Boundary Layer Theory, McGraw Hill, 1979.

[10] R.S. Gorla, Combined natural and forced convection in a laminar wall jet a long a vertical plates with uniform surface heat flux, Appl. Sci. Res. 31 (1976) 455–465.

[11] S.B. Savage, G.K. Chan, The buoyant two dimensional laminar vertical jets, Q. J. Mech. Appl. Math. 23 (1970) 413–430.

[12] G. Wilks, R. Hunt, The two-dimensional laminar vertical jet with positive or adverse buoyancy, Numer. Heat Tran. B (1985) 449–468.

[13] J.C. Mollendorf, B. Gebhart, Thermal buoyancy round laminar vertical jets, Int. J. Heat Mass Transfer 95 (1973) 121–123.

[14] W.S. Yu, H.T. Lin, H.C. Shih, Rigorous numerical solutions and correlations for two dimensional laminar buoyant jets, Int. J. Heat Mass Transfer 35 (1992) 1131–1141.

[15] O.G. Martynenko, V.N. Korovkin, Y.A. Sokovishin, The class of self-similar solutions for laminar buoyant jets, Int. J. Heat Mass Transfer 32 (1989) 2297–2307.

[16] R.S. Brand, F.J. Lahey, The heated laminar vertical jet, J. Fluid Mech. 29 (1967) 305–315.

[17] H. Mhiri, S. Golli, G. Le Palec, P. Bournot, Influence des conditions d'émission sur un écoulement de type jet plan laminaire isotherme ou chauffé, Revue générale de thermique 37 (1998) 898–910.

[18] S. Marzouk, H. Mhiri, G. Le Palec, P. Bournot, Numerical study of momentum and heat transfer in a pulsed laminar jet, Int. J. Heat Mass Transfer 46 (2003) 4319–4334.

[19] P.R. Kanna, M.K. Das, Conjugate forced convection heat transfer from a flat plate by laminar plane wall jet flow, Int. J. Heat Mass Transfer 48 (2005) 2896–2910.

[20] K.K. Raja, M.K. Das, P.R. Kanna, Transient study of buoyancy-assisted mixed convection in laminar plane wall jet flow, Int. Commun. Heat Mass Tran. 34 (2007) 809–819.

[21] G.P. Hammond, Profile analysis of heat/mass transfer across the plane wall jet, in: Proceeding of the 7th international Heat Transfer Conference, Munich, Germany, 1982, pp. 349–355.

[22] H. Mhiri, S. Habli, S. Golli, G. Le Palec, P. Bournot, Etude numérique des conditions d'émission sur un écoulement de type jet plan turbulent isotherme ou chauffé, Int. J. Therm. Sci. 38 (1999) 904–915.

[23] S. Habli, H. Mhiri, S. Golli, G. Le Palec, P. Bournot, Etude numérique des conditions d'émission sur un écoulement de type jet axisymétrique turbulent, Int. J. Therm. Sci. 40 (2001) 497–511.

[24] J. Kechiche, Application des modèles de turbulence à bas nombre de Reynolds pour l'étude des jets pariétaux turbulents, Ph.D. thesis, Université de la Méditerrannée, France, Université de Monastir, Tunisie, 2006.